JAERI-Research
2002-013

EVALUATION OF NEUTRON-INDUCED REACTIONS ON ^{236}Pu FOR JENDL-3.3

July 2002

Osamu IWAMOTO and Tsuneo NAKAGAWA

日本原子力研究所
Japan Atomic Energy Research Institute

本レポートは、日本原子力研究所が不定期に公刊している研究報告書です。
入手の問合わせは、日本原子力研究所研究情報部研究情報課（〒319-1195　茨城県那珂郡東海村）あて、お申し越し下さい。なお、このほかに財団法人原子力弘済会資料センター（〒319-1195　茨城県那珂郡東海村日本原子力研究所内）で複写による実費頒布を行っております。

This report is issued irregularly.
Inquiries about availability of the reports should be addressed to Research Information Division, Department of Intellectual Resources, Japan Atomic Energy Research Institute, Tokai-mura, Naka-gun, Ibaraki-ken 〒319-1195, Japan.

編集兼発行　日本原子力研究所

JAERI－Research 2002－013

Evaluation of Neutron-induced Reactions on ^{236}Pu for JENDL-3.3

Osamu IWAMOTO and Tsuneo NAKAGAWA

Department of Nuclear Energy System
Tokai Research Establishment
Japan Atomic Energy Research Institute
Tokai-mura, Naka-gun, Ibaraki-ken

(Received May 7, 2002)

Cross sections and energy-angular distributions of emitted neutrons were evaluated for the neutron-incident reactions on ^{236}Pu in the incident energy range of 10 eV to 20 MeV by using a statistical model combined with a coupled channel optical model. The calculated results were compiled to the latest evaluated nuclear data library JENDL-3.3 in the ENDF-6 format. The unresolved resonance region is assumed to be from 10 eV to 30 keV, and the averaged resonance parameters were obtained to reproduce the calculated cross sections. Maxwell temperatures for fission neutron spectra were estimated from a systematics with a correction for prefission neutrons.

Keywords: Nuclear Data Evaluation, ^{236}Pu Neutron Cross Sections, Statistical Model, Optical Model, Coupled Channel Calculation

JENDL-3.3のための^{236}Puの中性子入射反応の評価

日本原子力研究所東海研究所エネルギーシステム研究部
岩本 修 ・ 中川 庸雄

(2002年5月7日受理)

10 eVから20 MeVの入射中性子に対する^{236}Puの断面積と放出中性子の角度分布及びエネルギー分布を統計模型とチャンネル結合光学模型を用いて評価した。計算結果はENDF-6フォーマットに編集し評価済核データライブラリJENDL-3.3に格納した。10 eVから30 keVを非分離共鳴領域とし、断面積を再現する平均の共鳴パラメータを求めた。核分裂中性子のエネルギー分布を与えるMaxwell温度を計算した断面積を用いて系統式から推定した。

東海研究所：〒319-1195 茨城県那珂郡東海村白方白根2-4

Contents

目次

1 Introduction

Nuclear data for minor actinides are becoming important for purposes such as transmutation technology of long-lived radio-active wastes and high burn-up reactors. From recent measurments[1, 2] of neutron induced fission cross section for ^{236}Pu, however it becomes evident that the evaluated fission cross section in JENDL-3.2 is considerable underestimated below the incident neutron energy of 1 MeV. The present work was done to improve the fission cross section in JENDL-3.2.

A spherical optical model was used for the evaluation of ^{236}Pu in JENDL-3.2. However, for actinides, which show deformed feature making low-lying rotational excited levels, it is known that a coupled channel treatment is better. Thus we adopted the coupled channel optical model to evaluate ^{236}Pu cross sections. A statistical model calculation was performed in a consistent way to deduce the fission cross section, other reaction cross sections, and secondary neutron spectra and angular distributions. Detailes of the calculation are shown in Sect. 2. Results of the calculation are presented in Sect. 3 comparing with experimental data and other evaluated data.

2 Statistical Model Description

In this section, formulae and parameters used in the present calculation are shown. Neutron and γ-ray emissions and fission were taken into account as decay channels in the statistical model calculation. Details of the model for each decay channel are described below. The statistical model calculation was performed by the code GNASH[3].

In the present calculation continuum states for the compound neucleus were divided into energy bins of 0.05 to 0.1 MeV width, depending on the incident neutron energies. Preequilibrium processes were taken into account using the exciton model [3] with an interaction normalization constant k=160 MeV^3 and a single particle state density constant g=18.6.

2.1 Optical Model

The coupled channel (CC) method with a deformed optical potential was used to estimate transmission coefficients of the neutron channel in the Hauser-Feshbach statistical model, and also to calculate total, elastic scattering and direct-inelastic cross sections. For the CC calculation, the coupled channel optical model code OPTMAN[4] was used in the rigid rotor option. Four discrete levels in the ground state rotational band were included in the calculation. The optical model potential parameters were taken from a recent study for

^{238}U[5].

The deformed nuclear optical potential arises from deformed instant nuclear shapes

$$R(\theta', \varphi') = R_0 \left\{ 1 + \sum_{\lambda=2,4,6} \beta_{\lambda 0} Y_{\lambda 0}(\theta', \varphi') \right\}. \tag{1}$$

where $Y_{\lambda 0}$ means spherical harmonics, θ' and φ' angular cordinates in body-fixed system. The non-spherical optical potential is taken to a standard form:

$$\begin{aligned} V(r) &= -V_R f_R(r) + i \left\{ 4 W_D a_D \frac{d}{dr} f_D(r) - W_V \ f_V(r) \right\} \\ &\quad + \left(\frac{\hbar}{\mu_\pi c} \right)^2 V_{SO} \frac{1}{r} \frac{d}{dr} f_{SO}(r) \hat{\sigma} \cdot \hat{L}, \end{aligned} \tag{2}$$

with the form factors given as

$$f_i(r) = \left[1 + \exp\left(r - R_i \right) / a_i \right]^{-1}, \qquad i = R, V, D \ \text{and} \ SO, \tag{3}$$

and deformed radii R_i as described in Eq. (1) with $R_0 = r_i A^{1/3}$. The subscripts $i = R, V, D, Coul$ and SO denote the real volume, imaginary volume, imaginary surface, Coulomb and real spin-orbit potential, respectively. Energy dependence is given as

$$\begin{aligned} V_R &= V_R^0 + V_R^1 E_n + V_R^2 E_n^2 - C_{viso}(A - 2Z)/A, \\ W_D &= W_D^0 + W_D^1 E_n - C_{wiso}(A - 2Z)/A, \\ W_V &= W_V^0 + W_V^1 E_n \end{aligned} \tag{4}$$

where E_n is the incident energy of neutron and W_i^1 is changed at $E_n = E_{change}$, while Z and A denotes atomic and mass number of the target nucleus, respectively. If energy dependence lead to negative W_D or W_V values, they are set to zero for such energies.

The parameters and the levels used in the calculation is shown in Table 1 and 2, respectively.

2.2 Level Density

The Fermi gas level density formula given by Gilbert and Cameron[6] was used.

$$\rho(U, J, \pi) = \rho_\pi(\pi) \rho_J(J, U) \rho_U(U), \tag{5}$$

$$\rho_\pi(\pi) = \frac{1}{2}, \tag{6}$$

$$\rho_J(J, U) = \frac{2J + 1}{2\sigma^2} \exp \frac{-(J + \frac{1}{2})^2}{2\sigma^2}, \tag{7}$$

$$\rho_U(U) = \frac{1}{12\sqrt{2}\sigma U (aU)^{1/4}} \exp(2\sqrt{aU}), \tag{8}$$

where a is a level density parameter, and U is given by $U = E - \Delta$. E is an excitation energy and Δ is a paring energy. The level density parameter was obtained by the systematics[3],

$$a = [0.00917(S(Z) + S(N)) + 0.120]A, \tag{9}$$

where A is a mass number, $S(Z)$ and $S(N)$ are shell collections for proton and neutron, respectively. The spin cutoff parameter σ was given by

$$\sigma^2 = 0.146A^{2/3}\sqrt{aU}. \tag{10}$$

The $\rho_U(U)$ is an observable level density

$$\rho_U(U) = \sum_{J,\pi} \rho(U, J, \pi). \tag{11}$$

The Fermi gas level density is connected to constant temperature level density formula ρ_T at E_m.

$$\rho_T(U) = \frac{1}{T} \exp \frac{U + \Delta - E_0}{T}, \tag{12}$$

where T is a nuclear temperature, E_0 is a normalization constant. These parameters were determined to connect experimental low-lying levels at the excitation energy E_c and Fermi gas level density ρ_U at E_m, smoothly. A cumulative plot calculated with the obtained level density parameters for ^{237}Pu is shown in Fig. 1 with known excited levels. Parameters used in the calculation are given in Table 3. For the nuclei having no experimental excited level data, E_c and E_0 parameters were set equal to 0.

2.3 γ-transition

E1, M1 and E2 γ transitions were taken into account. Transmission coefficients of γ-ray are given by

$$T_{Xl}(\epsilon_\gamma) = 2\pi f_{Xl} \epsilon_\gamma^{2l+1}, \tag{13}$$

where ϵ_γ stands for the γ-ray energy, Xl denotes $E1$, $E2$ or $M1$, and f_{Xl} is a strength function of γ-ray. The strength function given by Kopecky and Uhl [7] was used for f_{Xl}. For the E1 transitions, the strength function is expressed by a sum of two Lorentzian forms with an energy dependent resonance width $\Gamma(\epsilon_\gamma)$ obtained from the Fermi liquids theory [8].

$$f_{E1} = \sum_{i=1,2} K_1 \left\{ \frac{\epsilon_\gamma \Gamma_i(\epsilon_\gamma)}{\left(\epsilon_\gamma^2 - E_i^2\right)^2 + \epsilon_\gamma^2 \Gamma_i(\epsilon_\gamma)^2} + \frac{0.7\Gamma_{i0} 4\pi^2 T^2}{E_i^5} \right\} \sigma_0^i \Gamma_{i0} \tag{14}$$

$$\Gamma_i(\epsilon_\gamma) = \Gamma_{i0} \frac{\epsilon_\gamma^2 + 4\pi^2 T^2}{E_i^2} \tag{15}$$

where Γ_{i0} and E_i are the width and energy of the i-th resonance, respectively. σ_0 is the strength parameter. Nuclear temperature T is given by

$$T = \sqrt{\frac{B_n - \epsilon_\gamma}{a}}, \tag{16}$$

where B_n is the neutron binding energy and a is given by Eq. (9). Giant dipole resonance (GDR) parameters for E1 transition are taken from Dietrich and Berman's table [9] assuming the same parameters as ^{238}U. The GDR parameters used in the calculation is shown in Table 4. The M1 and E2 strength functions, f_{M1} and f_{E2}, are given by single Lorentzian forms. The M1 strength function is expressed by

$$f_{M1} = K_1 \frac{\sigma_0 \epsilon_\gamma \Gamma^2}{\left(\epsilon_\gamma^2 - E^2\right)^2 + \epsilon_\gamma^2 \Gamma^2}, \tag{17}$$

with $E = 41/A^{1/3}$ (MeV), $\Gamma = 4$ (MeV) and $\sigma_0 = 1$ (mb). The E2 strength function is given by

$$f_{E2} = K_2 \frac{\sigma_0 \epsilon_\gamma^{-1} \Gamma^2}{\left(\epsilon_\gamma^2 - E^2\right)^2 + \epsilon_\gamma^2 \Gamma^2} \tag{18}$$

where resonance parameters were obtained from a systematics by Prestwich et al. [10]: $E = 63/A^{1/3}$ (MeV), $\Gamma = 6.11 - 0.012A$ (MeV) and $\sigma_0 = 1.5 \times 10^{-4} Z^2 E^2 A^{-1/3}/\Gamma$ (mb). Constant K_l ($l = 1$ or 2) in the strength functions is given by

$$K_l = \frac{1}{(2l+1)\pi^2 \hbar^2 c^2}. \tag{19}$$

Absolute values of the E1 strength function were obtained by multiplying a normalization factor which can be determined to reproduce experimental $2\pi\langle\Gamma_{\gamma 0}\rangle/\langle D_0\rangle$ value with integrating the E1 transition strength at neutron binding energy for the compound nucleus. However, since no experimental resonance data were available to evaluate $2\pi\langle\Gamma_{\gamma 0}\rangle/\langle D_0\rangle$, the value of $2\pi\langle\Gamma_{\gamma 0}\rangle/\langle D_0\rangle$ was assumed to be 0.02 for ^{237}Pu, 0.5 for ^{236}Pu, 0.01 for ^{235}Pu and 0.5 for ^{234}Pu. The E2 and M1 strength functions were normalized by multiplying the normarization factor of $R(Ml)/R(El) = 0.45/(r_0 A^{1/3})^2$ and $R(El+1)/R(El) = 8 \times 10^{-4}$, where $R(Xl)$ is relative strength[3].

2.4 Fission

The fission transmission coefficient was calculated by assuming double parabolic fission barrier with Hill-Wheeler's expression[11].

$$T = \frac{1}{1 + \exp\left\{-\frac{2\pi}{\hbar\omega}(U - E_b)\right\}} \tag{20}$$

where E_b and $\hbar\omega$ are fission barrier height and curvature, respectively. Fission reactions were assumed to occur through discrete levels and continuum states at the saddle points of fission barriers. In the present work the discrete transition levels were produced assuming rotational bands. Giving band head energies and a moment of inertia, 10 rotational levels were produced for each band. Above the discrete levels, continuum level densities were assumed to be given by the formulae described in Sect. 2.2. The fission barrier parameters and band head data used are shown in Table 5 and and also the parameters used in the level density formula are given in Table 6. The E_i^{band} and J_i^{π} indicate energy and spin-parity of the i-th band head for the discrete fission transition levels, respectively. Fission barrier parameters were determined to reproduce experimental fission cross sections [1, 2].

3 Results

In this section calculated cross sections and energy spectra are shown together with experimental data and other evaluated data. Other quantities required for an evaluated nuclear data file are also described.

3.1 Cross Sections

The resolved resonance energy region was assumed to be below 10 eV and the unresolved resonance energy region from 10 eV to 30 keV. In the resolved energy region, resonance parameters were taken from ENDF/B-VI evaluated data file because they reproduce well experimental fission cross section [1, 2, 12, 13] both at the thermal energy and in the resolved resonace energy region. In the unresolved resonance region, resonance parameters were determined to reproduce the calculated cross sections assuming s- and p-wave resonances. The calculation was performed by the unresolved parameter search code ASREP[14], in which a single Breit-Wigner resonance formula is used with a Wigner distribution for the level spacing and a Porter-Thomas distribution for the level width fluctuation.

Figure 2 shows the results of total, elastic scattering and reaction cross sections calculated with the coupled channel optical model. Calculated s- and p-wave neutron strength functions at 1 eV are 1.08×10^{-4} and 2.11×10^{-4}, respectively. Comparisons of the total cross section with the evaluated data in JENDL-3.2, ENDF/B-VI and JEF-2.2 are shown in Figs. 3 and 4. The present calculated total cross section is smaller than JENDL-3.2 in the whole energy region and almost the same as the ENDF/B-VI at higher energies than 2 MeV. As shown in Figs. 5 and 6, in the case of the elastic scattering cross section the present calculation is the smallest above 2 MeV. In the lower energy region, the present result is similar to JEF-2.2,

a little bit larger than ENDF/B-VI and considerably smaller than JENDL-3.2. The capture cross section is shown in Fig. 7. The present result is the smallest below 100 keV among the evaluated data and above this energy between JEF-2.2 and JENDL-3.2.

The result of fission cross section is shown in Figs. 8 and 9 with available experimental data [1, 2, 12, 13] in the experimental nuclear reaction data library EXFOR and evaluated data. The present result reproduces the experimental data at 10 to 100 eV and above 1 MeV well. In unresolved resonance energy region, the present calculation is smaller than experimental data. However, it is difficult to reproduce this large fission cross section using reasonable optical model and statistical model parameters expected from neighboring nuclei at present.

Cross sections for the (n,n'), (n,2n) and (n,3n) reactions are shown in Fig. 10. The present (n,n') calculation gives the largest value. The (n,2n) and (n,3n) cross sections are between JEDNL-3.2 and JEF-2.2 (the same as ENDF/B-VI).

3.2 Angular Distributions

The angular distributions of secondary neutrons were calculated for the elastic and inelastic scattering cross sections by summing the direct, preequilibrium and compound reaction components. The direct and compound reaction components were obtained by the optical model and Hauser-Feshbach calculation, respectively. The preequilibrium components were estimated by the systematics of Kalbach[15], assuming that all preequilibrium components are multistep direct parts because the present exciton calculation does not distinguish the bound and unbound particle states. For the (n,2n), (n,3n), and fission reactions, isotropic angular distributions were assumed.

3.3 Energy Distributions

The energy distributions of emitted neutrons for each reaction were obtained by summing neutron emission spectra multiplied by probabilities of specific reaction channels from every excited states neglecting spin distributions. Figures 11, 12, and 13 show secondary neutron energy distributions emitted from the (n,n'), (n,2n), and (n,3n) reactions, respectively.

The fission neutron spectra were estimated by assuming Maxwellian distributions with the temperature T_m given by the systematics of Howerton and Doyas[16].

$$T_m = c + d\sqrt{1 + \nu_f(E)}, \tag{21}$$
$$c = 0.353, \quad d = 0.510$$

where $\nu_f(E)$ is an average number of neutrons per fission after scission at incident energy E. The $\nu_f(E)$ value is taken from JENDL-3.2 with subtracting the prefission neutron number for second and third chance fissions multiplying the ratio of their cross sections obtained by the present statistical model calculation. The incident energy dependence of T_m is shown in Fig. 14. A plateau can be seen around the threshold of second chance fission. Fission neutron spectra at incident energies of 1 eV, 1 keV, 1 MeV, 10 MeV and 20 MeV are shown in Fig. 15.

3.4 Number of Neutrons Per Fission

To complete an evaluated nuclear data file as the ENDF-6 format, the number of neutron per fission ν for prompt and delayed neutron emission are required. In the present work ν_p and ν_d were taken from JENDL-3.2.

4 Conclusion

The nuclear data for ^{236}Pu was evaluated based on the statistical model. Details of the calculation were described and the results were compared with experimental data and other evaluated data. All of cross sections, secondary neutron energy distributions and angular distributions were revised for JENDL-3.3 by the present work. In particular, the fission cross section is in better agreement with experimental data. compared to JENDL-3.2

Acknowledgments

Authors are greateful to Dr. Akira Hasegawa and other members of Nuclear Data Center for helpful comments on this work.

References

[1] E. A. Gromova, S. S. Kovalenko, Yu. A. Selitskii, A. M. Fridkin, V. B. Funshtein, V. A. Yakovlev, S. V. Antipov, P. E. Vorotnikov, B. M. Gokhberg, V. V. Danichev, V. N. Dement'ev, V. S. Zenkevich, S. A. Isakov: Sov. Atom. Ener. **68**, 223 (1990) EXFOR 41064

[2] P. E. Vorotnikov, B. M. Gokheerg, E. A. Gromova, S. S. Kovalenko, Yu. A. Selitskiy, A. M. Fridkin, V. B. Funshtein, V. A. Yakovlev: *"Proceedings of 1st. Int. Conf. on Neutron Physics"*, Kiev, 14-18 Sep 1987, Vol. 3, 76 (1987) EXFOR 40992

[3] P. G. Young, E. D. Arthur, M. B. Chadwick: *"Proceedings of the Workshop Nuclear Reaction Data and Nuclear Reactors - Physics, Design and Safety - "*, Trieste, Vol. 1, p. 227 (1998) World Scientific

[4] E. Sh. Sukhovitskiĭ, Y. V. Porodzinskiĭ, O. Iwamoto, S. Chiba, K. Shibata: "*Programs OPTMAN and SHEMMAN version 5 (1998)*", JAERI-Data/Code 98-019 (1998)

[5] E. Sh. Sukhovitskiĭ, O. Iwamoto, S. Chiba, T. Fukahori: J. Nucl. Sci. Technol., **37**, 120 (2000)

[6] A. Gilbert, A. G. W. Cameron: Canadican J. Phys. **43**, 1446 (1965)

[7] J. Kopecky, M. Uhl: Phys. Rev. **C41**, 1941 (1990)

[8] S. G. Kadmenskiĭ, V. P. Markushev, V. I. Furman: Sov. J. Nucl. Phys. **37**, 165 (1983)

[9] S. S. Dietrich, B. L. Berman: Atomic Data and Nuclear Data Tables **38**, 199 (1988)

[10] W. V. Prestwich, M. A. Islam, T. J. Kennett: Z. Phys. A **315**, 103(1984)

[11] D. L. Hill, J. A. Wheeler: Phys. Rev. **89**, 1102 (1953)

[12] B. N. Belyaev, E. A. Gromova, V. N. Dement'ev, V. S. Zenkevich, A. V. Lovtsyus, Yu. A. Selitskii, A. M. Fridkin, V. B. Funshtein, V. A. Yakovlev: Sov. Atom. Ener. **68**, 332 (1990) EXFOR 41093

[13] J. E. Gindler, J. Gray Jr., J. R. Huizenga: Phys. Rev. **115**, 1271 (1959) EXFOR 13572

[14] Y. Kikuchi, T. Nakagawa, Y. Nakajima: *"ASREP: A computer Program for Automatic Search of Unresolved Resonance Parameters"*, JAERI-Data/Code 99-025 (1999) (in Japanese)

[15] C. Kalbach: Phys. Rev. **C37**, 2350 (1988)

[16] R.J. Howerton, R.J. Doyas: Nucl. Sci. Eng. **46**, 414 (1971)

Table 1: Optical potential parameters used in the calculation

$V_R = 46.65 - 0.307E + 0.001E^2$

$$W_D = \begin{cases} 4.49 + 0.491E & E \leq 11.2 \\ 9.99 - 0.071(E - 11.2) & E > 11.2 \end{cases}$$

$$W_V = \begin{cases} 0.0 & E \leq 11.2 \\ 0.100(E - 11.2) & E > 11.2 \end{cases}$$

$V_{SO} = 6.02$

$r_R = 1.2616$ $\quad a_R = 0.643$

$r_D = 1.2331$ $\quad a_D = \begin{cases} 0.567 + 0.0022E & E \leq 11.2 \\ 0.5916 & E > 11.2 \end{cases}$

$r_V = 1.245$ $\quad a_V = 0.324$

$C_{viso} = 5.0$ $\quad C_{wiso} = 9.0$

$r_{SO} = 1.12$ $\quad a_{SO} = 0.59 - 0.002E$

$\beta_{20} = 0.219$ $\quad \beta_{40} = 0.053$ $\quad \beta_{60} = -0.0065$

Potential strength and incident energy E in MeV; radii and diffusenesses in fm.

Table 2: Levels of ^{236}Pu used in the coupled channel calculation

J^π	Ex (MeV)
0.0	0^+
0.04463	2^+
0.14745	4^+
0.30580	6^+
0.5157	8^+

Table 3: Parameters used in the level density formulae

	a (/MeV)	T (MeV)	Δ (MeV)	E_m (MeV)	E_c (MeV)	E_0
^{237}Pu	26.332	0.449	0.650	4.501	0.4606	-0.887
^{236}Pu	25.961	0.451	1.350	5.149	0.6207	-0.143
^{235}Pu	25.937	0.384	0.750	3.297	0.0000	0.000
^{234}Pu	26.020	0.435	1.310	4.807	0.0000	0.000
^{233}Pu	26.058	0.379	0.710	3.177	0.0000	0.000

Table 4: GDR parameters for γ transition

	σ_0^1 (b)	E_1 (MeV)	Γ_1 (MeV)	σ_0^2	E_2 (MeV)	Γ_2 (MeV)
E1	0.3	10.77	2.37	0.443	13.8	5.13
M1	1.0	6.62	4.0			
E2	6.83	10.18	3.27			

Table 5: Fission barrier parameters

		E_b (MeV)	$\hbar\omega$ (MeV)	E_1^{band} (MeV)	J_1^π	E_2^{band} (MeV)	J_2^π
^{237}Pu	inner	6.0	0.7	0.0	$\frac{1}{2}^+$	0.0	$\frac{1}{2}^-$
	outer	5.8	0.6	0.0	$\frac{1}{2}^+$	0.0	$\frac{1}{2}^-$
^{236}Pu	inner	6.0	0.7	0.0	0^+	0.5	2^+
	outer	5.8	0.6	0.0	0^+	0.5	2^+
^{235}Pu	inner	5.6	0.7	0.0	$\frac{1}{2}^+$	0.0	$\frac{1}{2}^-$
	outer	5.4	0.6	0.0	$\frac{1}{2}^+$	0.0	$\frac{1}{2}^-$

$\hbar^2/2I = 0.002$ (MeV) for all bands. I is a moment of inertia at the saddle point of fissin barrier.

Table 6: Level density parameters for fission transition states

	a (/MeV)	T (MeV)	Δ (MeV))	E_m (MeV)	E_c (MeV)	E_0
^{237}Pu	26.332	0.474	0.650	5.036	0.2400	-1.226
^{236}Pu	25.961	0.485	1.350	5.877	0.7080	-0.604
^{235}Pu	25.937	0.490	0.750	5.385	0.2400	-1.274

Level density enhancement factor [3] 6.0 is used for the inner barrier of ^{237}Pu and 2.0 for other barriers.

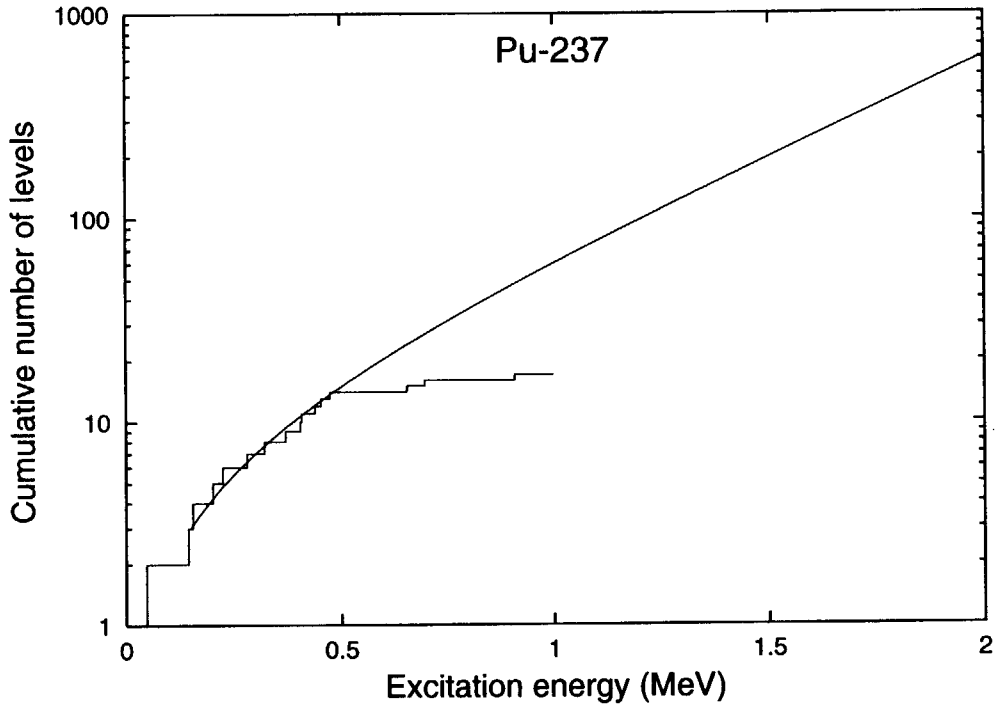

Fig. 1: Cumulative plot of level density and experimental levels for ^{237}Pu. Smoothed line is given by level density formula and staircase plot by experimental levels.

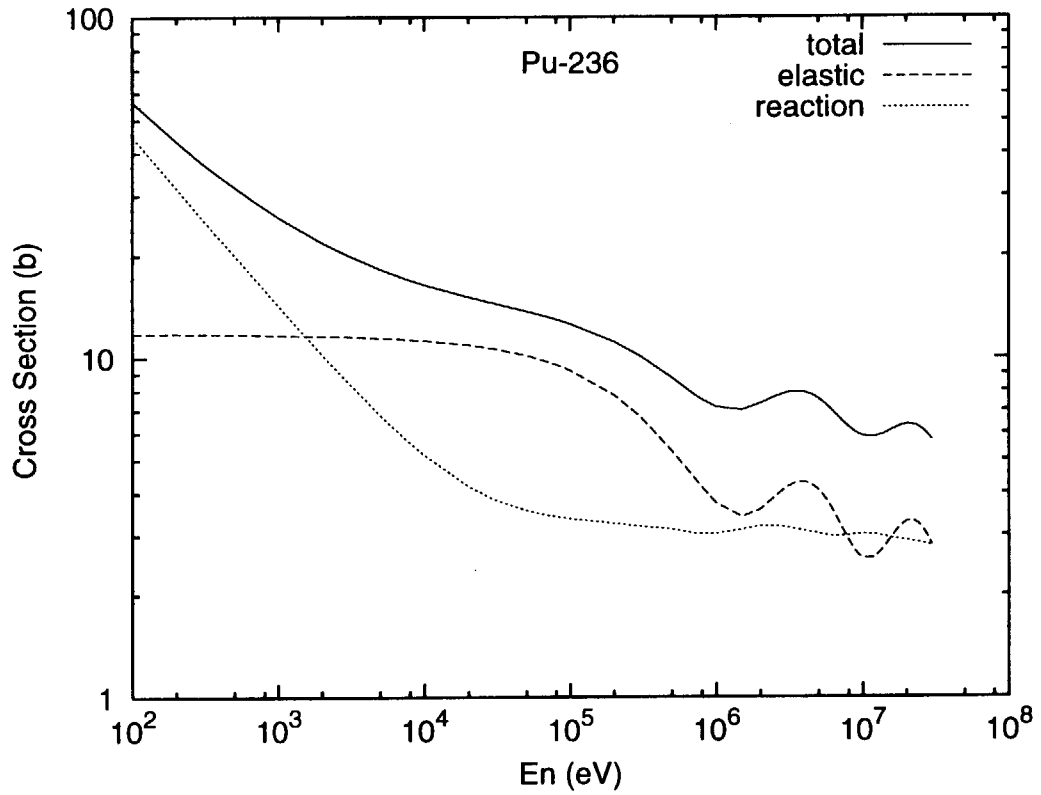

Fig. 2: Resutls of total, elastic and reaction cross sections calculated by a coupled channel optical model

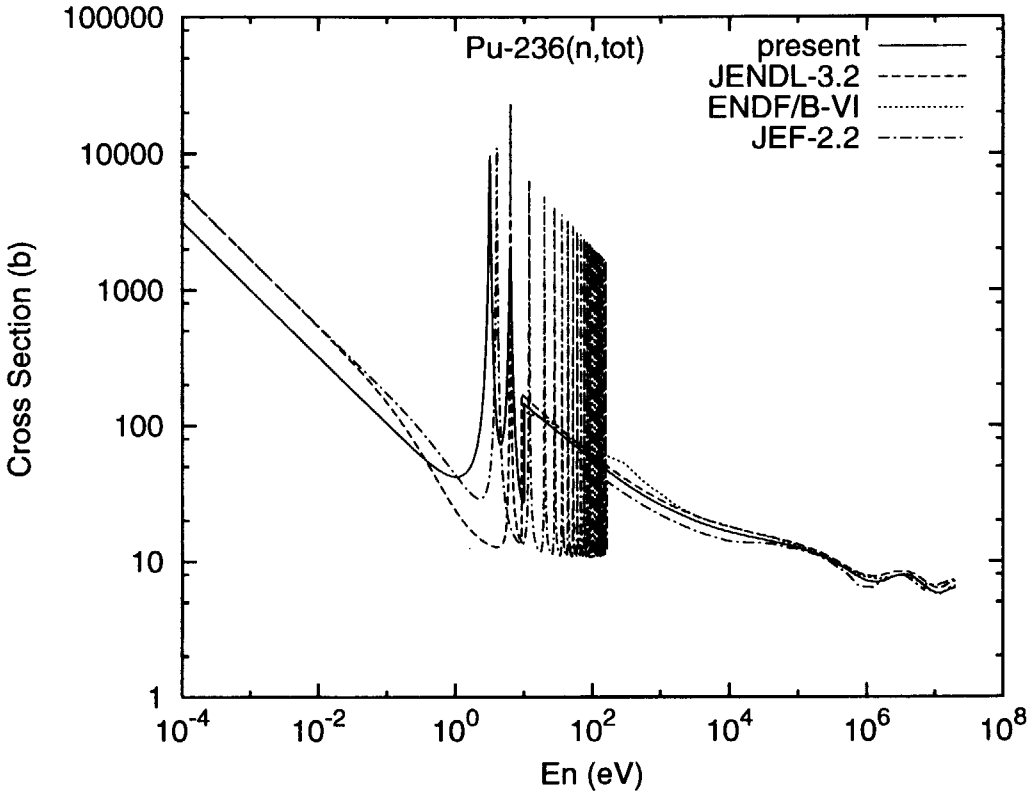

Fig. 3: Comparison of total cross section

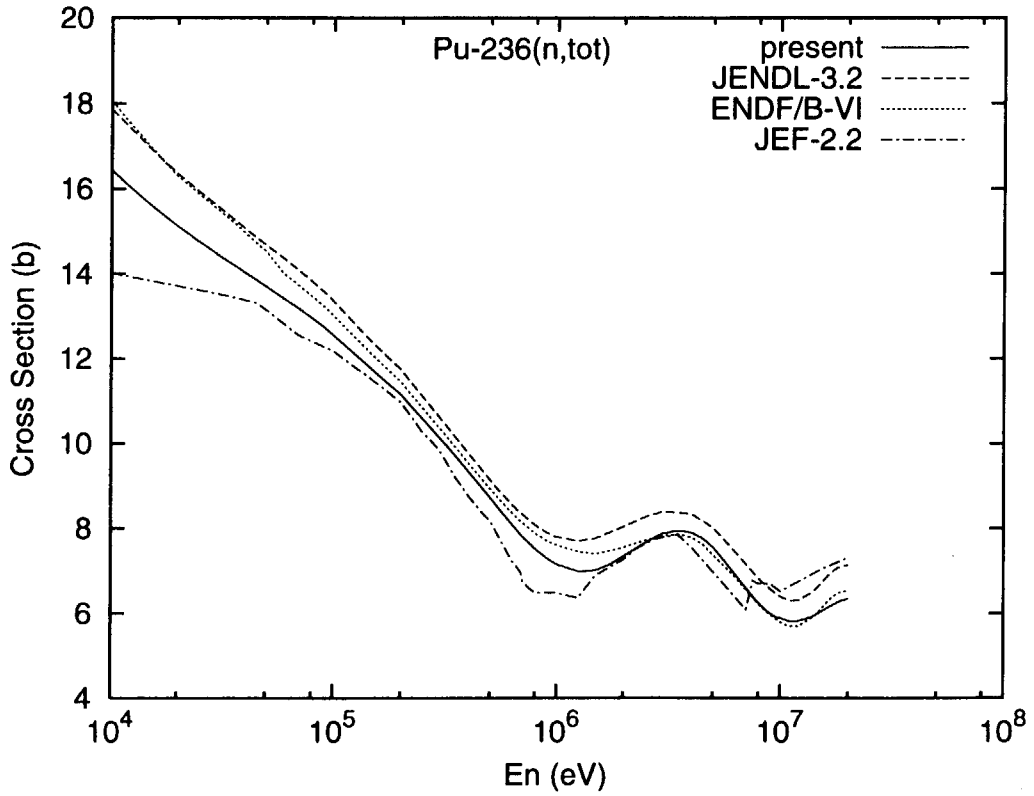

Fig. 4: Comparison of total cross section

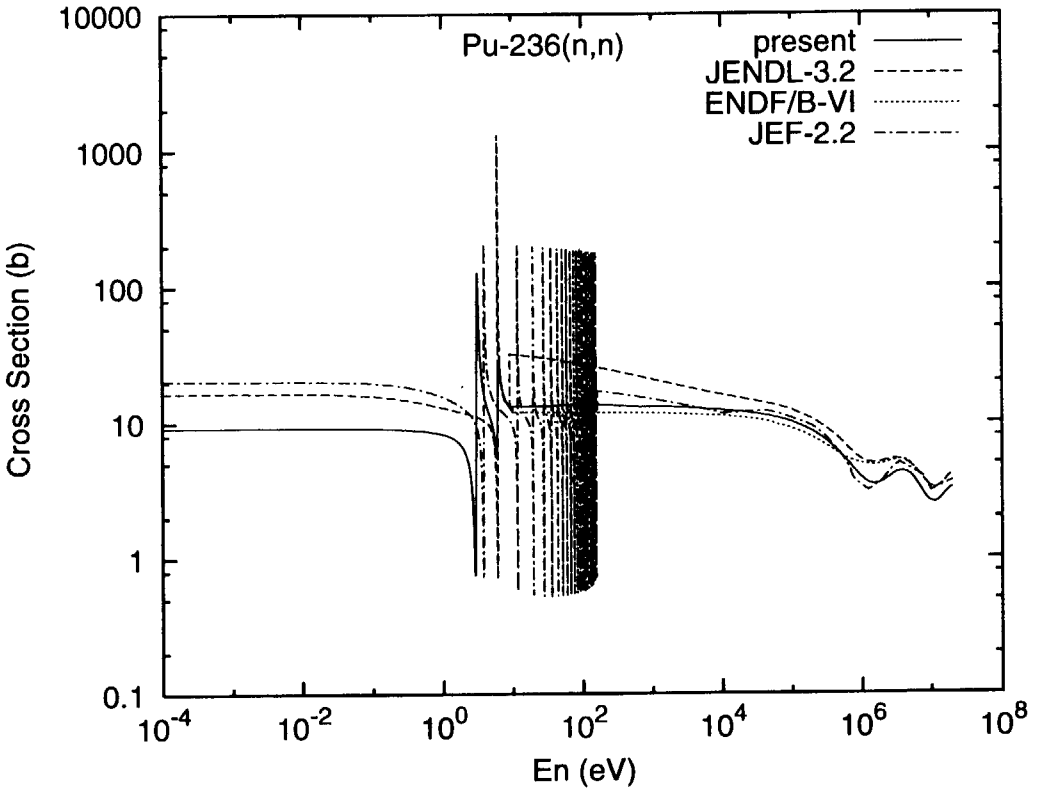

Fig. 5: Comparison of elastic scattering cross section

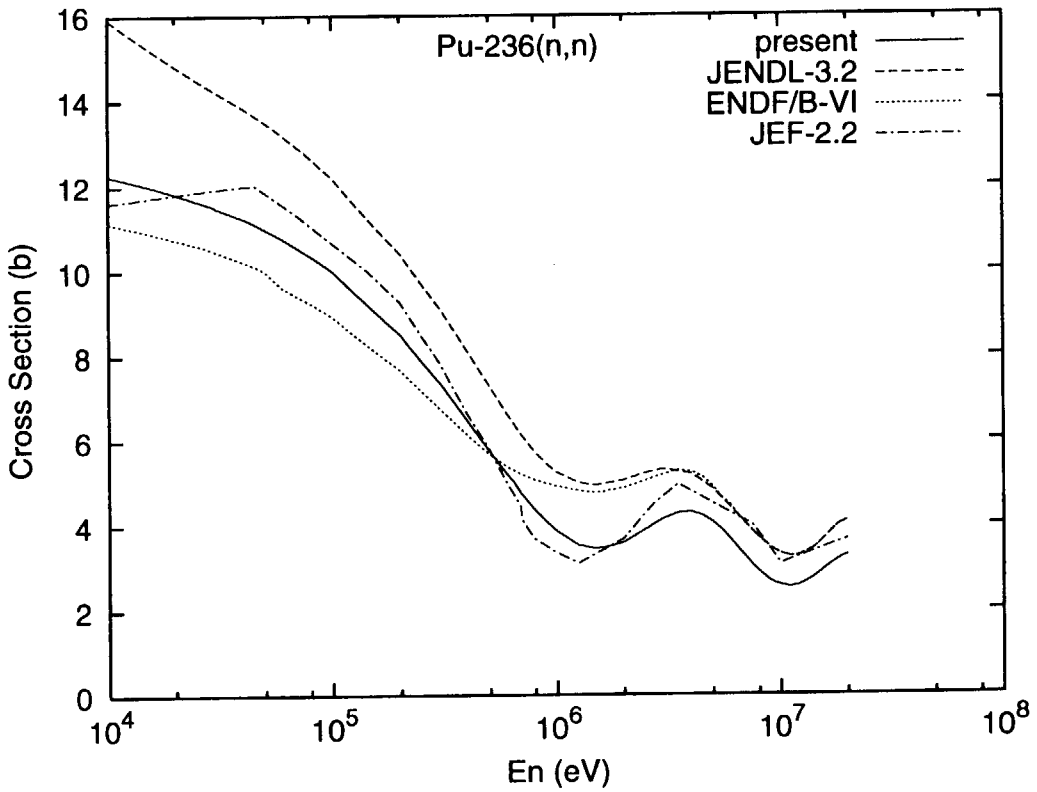

Fig. 6: Comparison of elastic scattering cross section

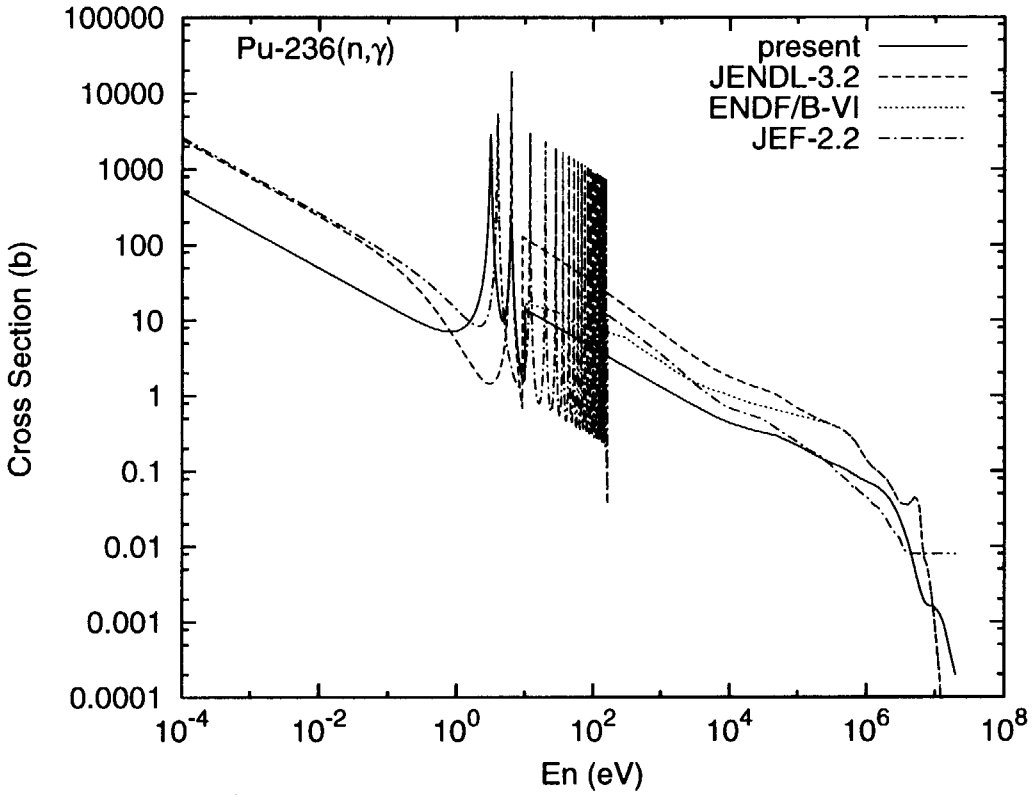

Fig. 7: Comparison of capture cross section

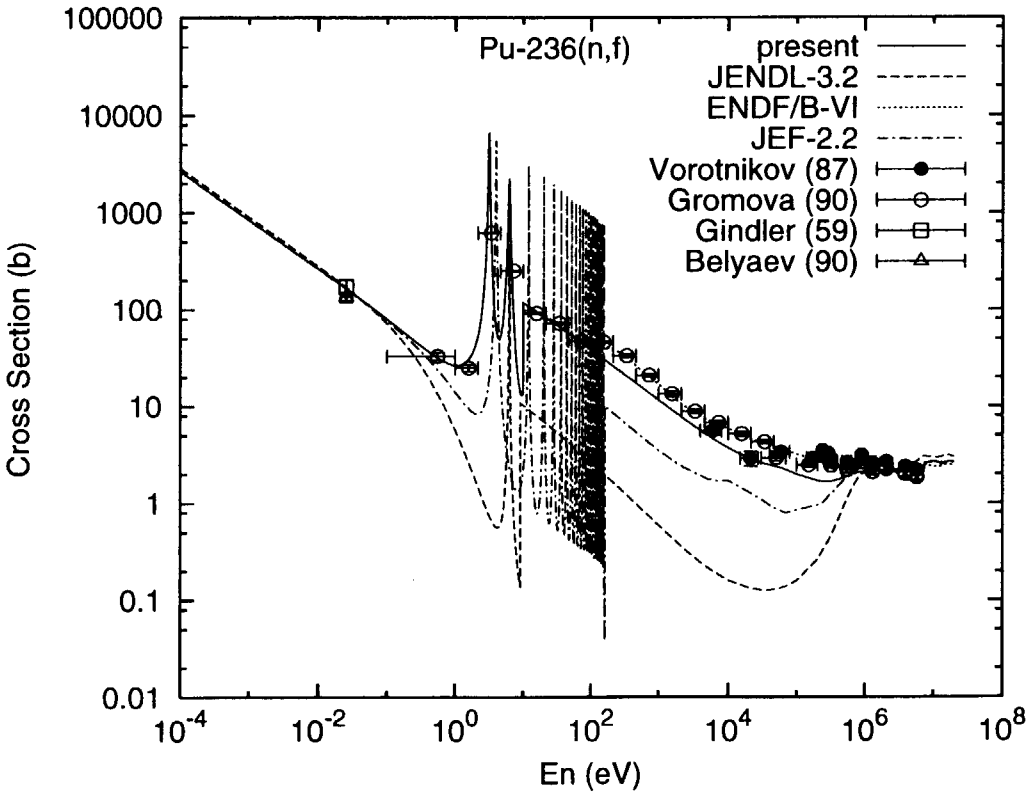

Fig. 8: Comparison of fission cross section

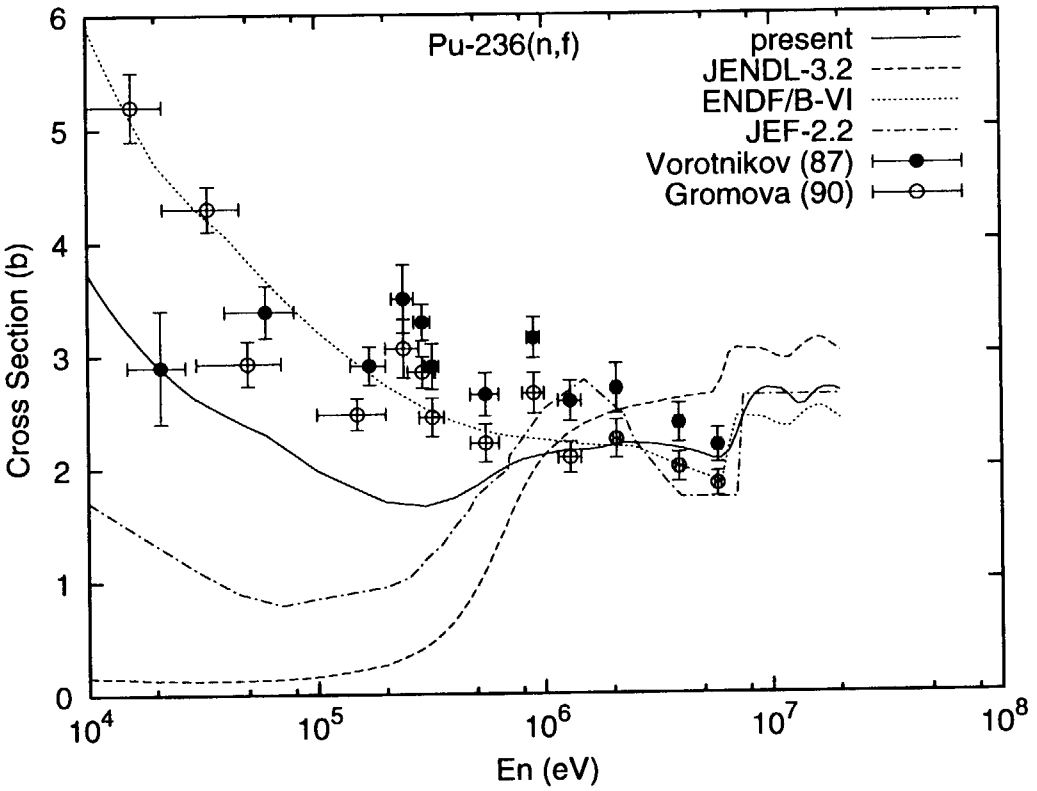

Fig. 9: Comparison of fission cross section

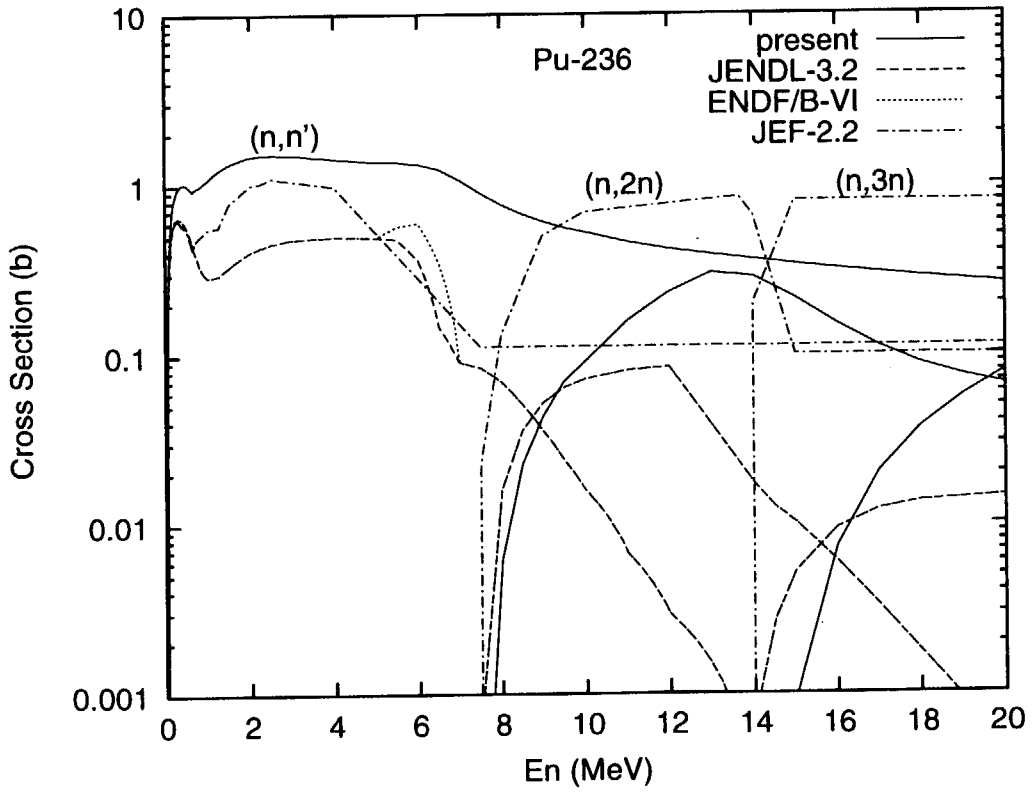

Fig. 10: Comparison of cross sections for (n,n'), (n,2n) and (n,3n) reactions

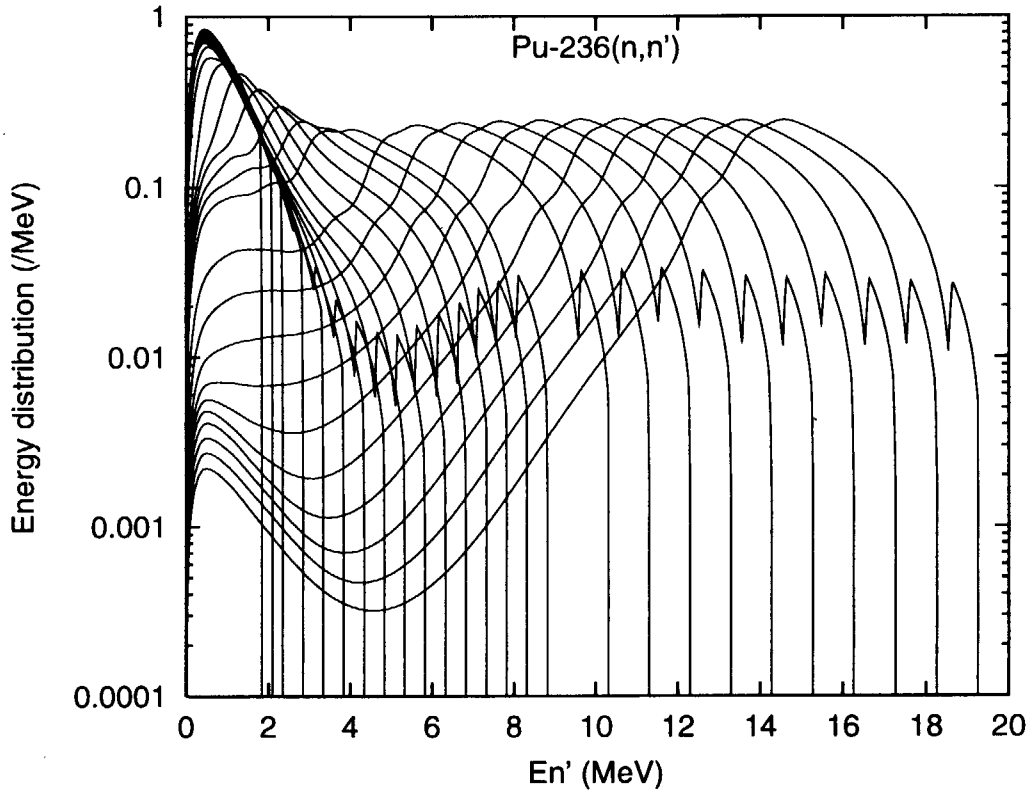

Fig. 11: Neutron energy spectrum from (n,n') reaction

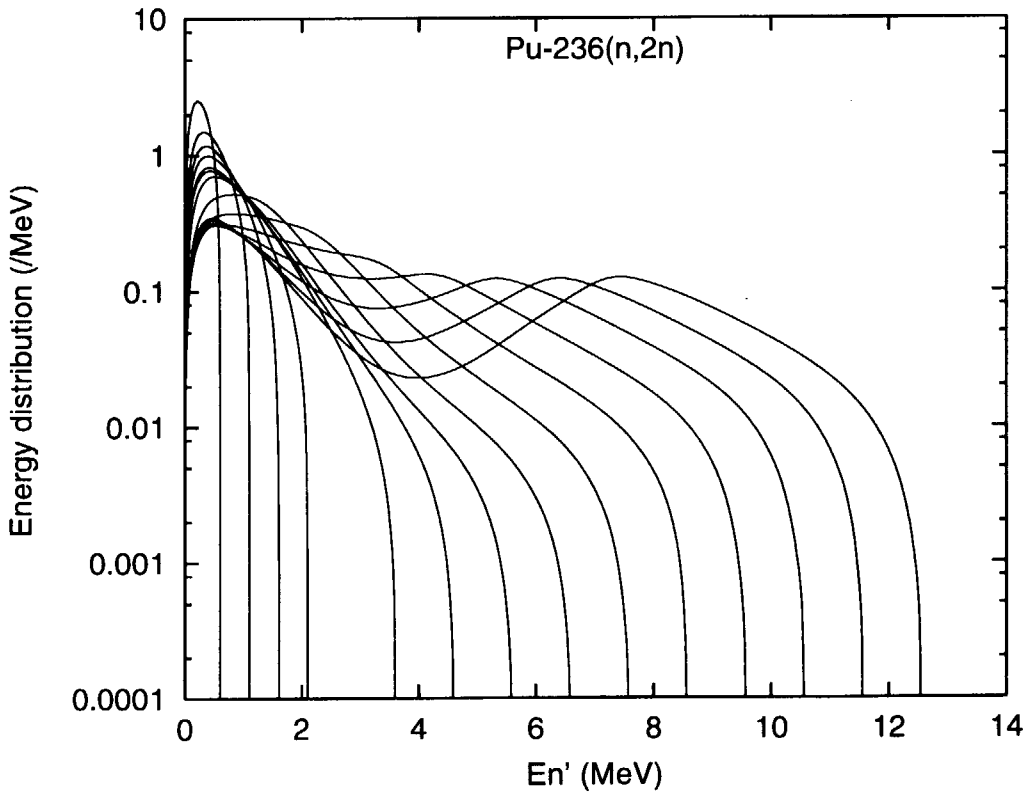

Fig. 12: Neutron energy spectrum from (n,2n) reaction

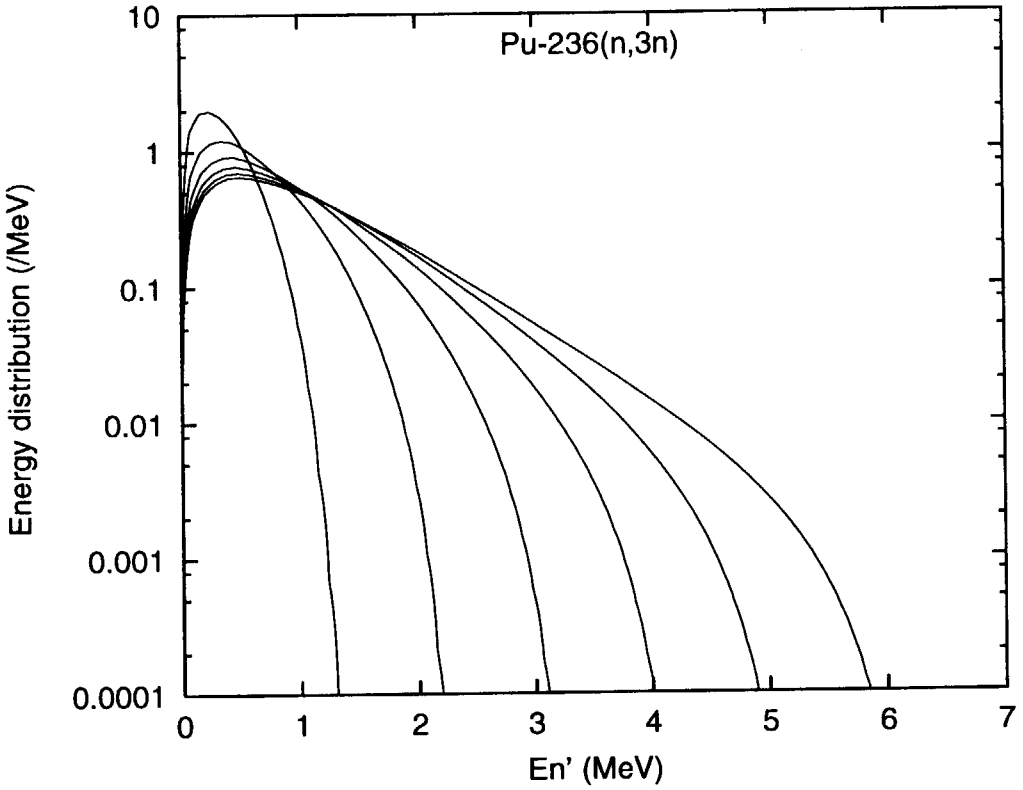

Fig. 13: Neutron energy spectrum from (n,3n) reaction

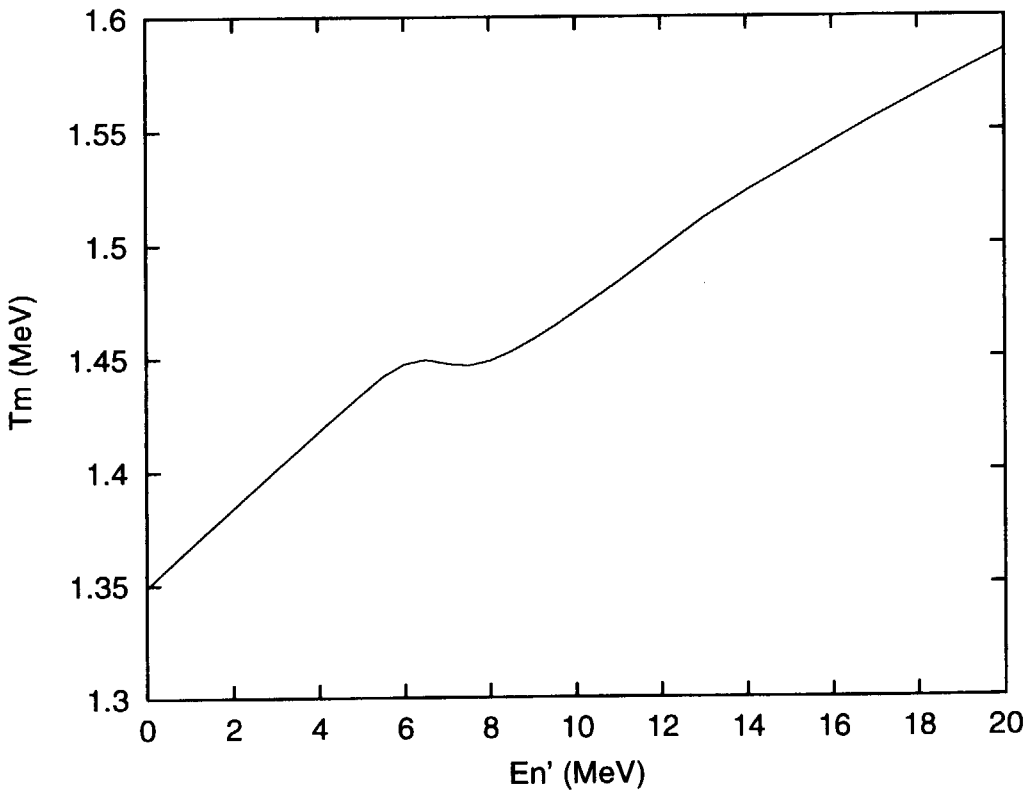

Fig. 14: Maxwell temperature for fisson neutron spectrum

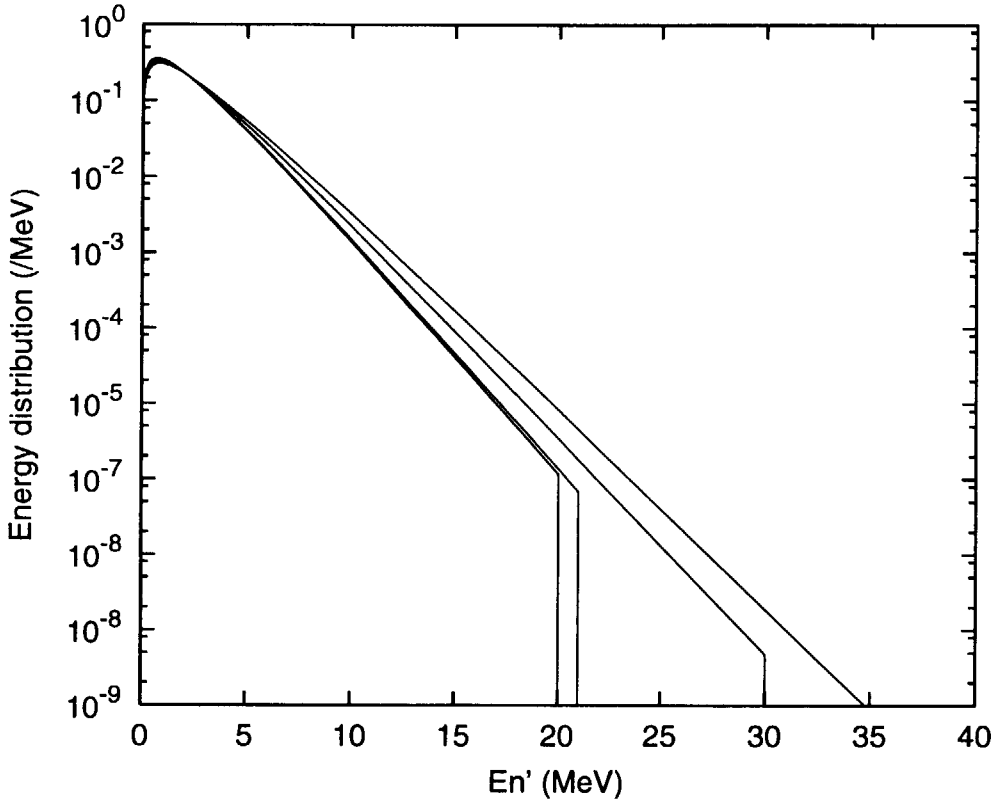

Fig. 15: Fission neutron energy spectra at the neutron incident energies of 1 eV, 1 keV, 1 MeV, 10 MeV and 20 MeV, upper cuttoff is located at $E'_n = E_n + 20$ MeV

国際単位系 (SI) と換算表

表 1　SI基本単位および補助単位

量	名称	記号
長さ	メートル	m
質量	キログラム	kg
時間	秒	s
電流	アンペア	A
熱力学温度	ケルビン	K
物質量	モル	mol
光度	カンデラ	cd
平面角	ラジアン	rad
立体角	ステラジアン	sr

表 2　SIと併用される単位

名称	記号
分，時，日	min，h，d
度，分，秒	°，′，″
リットル	l，L
トン	t
電子ボルト	eV
原子質量単位	u

1 eV = 1.60218 × 10^{-19} J

1 u = 1.66054 × 10^{-27} kg

表 5　SI接頭語

倍数	接頭語	記号
10^{18}	エクサ	E
10^{15}	ペタ	P
10^{12}	テラ	T
10^{9}	ギガ	G
10^{6}	メガ	M
10^{3}	キロ	k
10^{2}	ヘクト	h
10^{1}	デカ	da
10^{-1}	デシ	d
10^{-2}	センチ	c
10^{-3}	ミリ	m
10^{-6}	マイクロ	μ
10^{-9}	ナノ	n
10^{-12}	ピコ	p
10^{-15}	フェムト	f
10^{-18}	アト	a

表 3　固有の名称をもつSI組立単位

量	名称	記号	他のSI単位による表現
周波数	ヘルツ	Hz	s^{-1}
力	ニュートン	N	m·kg/s^2
圧力，応力	パスカル	Pa	N/m^2
エネルギー，仕事，熱量	ジュール	J	N·m
工率，放射束	ワット	W	J/s
電気量，電荷	クーロン	C	A·s
電位，電圧，起電力	ボルト	V	W/A
静電容量	ファラド	F	C/V
電気抵抗	オーム	Ω	V/A
コンダクタンス	ジーメンス	S	A/V
磁束	ウェーバ	Wb	V·s
磁束密度	テスラ	T	Wb/m^2
インダクタンス	ヘンリー	H	Wb/A
セルシウス温度	セルシウス度	℃	
光束	ルーメン	lm	cd·sr
照度	ルクス	lx	lm/m^2
放射能	ベクレル	Bq	s^{-1}
吸収線量	グレイ	Gy	J/kg
線量当量	シーベルト	Sv	J/kg

表 4　SIと共に暫定的に維持される単位

名称	記号
オングストローム	Å
バーン	b
バール	bar
ガル	Gal
キュリー	Ci
レントゲン	R
ラド	rad
レム	rem

1 Å = 0.1 nm = 10^{-10} m

1 b = 100 fm^2 = 10^{-28} m^2

1 bar = 0.1 MPa = 10^5 Pa

1 Gal = 1 cm/s^2 = 10^{-2} m/s^2

1 Ci = 3.7 × 10^{10} Bq

1 R = 2.58 × 10^{-4} C/kg

1 rad = 1 cGy = 10^{-2} Gy

1 rem = 1 cSv = 10^{-2} Sv

（注）

1. 表1－5は「国際単位系」第5版，国際度量衡局 1985年刊行による。ただし，1 eVおよび1 uの値はCODATAの1986年推奨値によった。
2. 表4には海里，ノット，アール，ヘクタールも含まれているが日常の単位なのでここでは省略した。
3. barは，JISでは流体の圧力を表わす場合に限り表2のカテゴリーに分類されている。
4. EC閣僚理事会指令ではbar，barnおよび「血圧の単位」mmHgを表2のカテゴリーに入れている。

換算表

力	N(=10^5 dyn)	kgf	lbf
	1	0.101972	0.224809
	9.80665	1	2.20462
	4.44822	0.453592	1

粘度　1 Pa·s(N·s/m^2) = 10 P(ポアズ)(g/(cm·s))

動粘度　1 m^2/s = 10^4 St(ストークス)(cm^2/s)

圧力	MPa(=10 bar)	kgf/cm^2	atm	mmHg(Torr)	lbf/in^2(psi)
	1	10.1972	9.86923	7.50062 × 10^3	145.038
	0.0980665	1	0.967841	735.559	14.2233
	0.101325	1.03323	1	760	14.6959
	1.33322 × 10^{-4}	1.35951 × 10^{-3}	1.31579 × 10^{-3}	1	1.93368 × 10^{-2}
	6.89476 × 10^{-3}	7.03070 × 10^{-2}	6.80460 × 10^{-2}	51.7149	1

エネルギー・仕事・熱量	J(=10^7 erg)	kgf·m	kW·h	cal(計量法)	Btu	ft·lbf	eV
	1	0.101972	2.77778 × 10^{-7}	0.238889	9.47813 × 10^{-4}	0.737562	6.24150 × 10^{18}
	9.80665	1	2.72407 × 10^{-6}	2.34270	9.29487 × 10^{-3}	7.23301	6.12082 × 10^{19}
	3.6 × 10^6	3.67098 × 10^5	1	8.59999 × 10^5	3412.13	2.65522 × 10^6	2.24694 × 10^{25}
	4.18605	0.426858	1.16279 × 10^{-6}	1	3.96759 × 10^{-3}	3.08747	2.61272 × 10^{19}
	1055.06	107.586	2.93072 × 10^{-4}	252.042	1	778.172	6.58515 × 10^{21}
	1.35582	0.138255	3.76616 × 10^{-7}	0.323890	1.28506 × 10^{-3}	1	8.46233 × 10^{18}
	1.60218 × 10^{-19}	1.63377 × 10^{-20}	4.45050 × 10^{-26}	3.82743 × 10^{-20}	1.51857 × 10^{-22}	1.18171 × 10^{-19}	1

1 cal = 4.18605 J (計量法)

= 4.184 J (熱化学)

= 4.1855 J (15 °C)

= 4.1868 J (国際蒸気表)

仕事率　1 PS (仏馬力)

= 75 kgf·m/s

= 735.499 W

放射能	Bq	Ci
	1	2.70270 × 10^{-11}
	3.7 × 10^{10}	1

吸収線量	Gy	rad
	1	100
	0.01	1

照射線量	C/kg	R
	1	3876
	2.58 × 10^{-4}	1

線量当量	Sv	rem
	1	100
	0.01	1

（86年12月26日現在）

Evaluation of Neutron-Induced Reactions on ^{236}Pu for JENDL-3.3